AD

TECHNICAL REPORT ARCCB-TR-98015

USE OF THE INSTRUMENTED BOLT AND CONSTANT DISPLACEMENT BOLT-LOADED SPECIMEN TO MEASURE IN SITU HYDROGEN CRACK GROWTH IN HIGH STRENGTH STEELS

19980921 059

GREGORY N. VIGILANTE
JOHN H. UNDERWOOD
DANIEL CRAYON

AUGUST 1998

**US ARMY ARMAMENT RESEARCH,
DEVELOPMENT AND ENGINEERING CENTER**
CLOSE COMBAT ARMAMENTS CENTER
BENÉT LABORATORIES
WATERVLIET, N.Y. 12189-4050

BENÉT
LABS

DISCLAIMER

The findings in this report are not to be construed as an official Department of the Army position unless so designated by other authorized documents.

The use of trade name(s) and/or manufacturer(s) does not constitute an official indorsement or approval.

DESTRUCTION NOTICE

For classified documents, follow the procedures in DoD 5200.22-M, Industrial Security Manual, Section II-19 or DoD 5200.1-R, Information Security Program Regulation, Chapter IX.

For unclassified, limited documents, destroy by any method that will prevent disclosure of contents or reconstruction of the document.

For unclassified, unlimited documents, destroy when the report is no longer needed. Do not return it to the originator.

REPORT DOCUMENTATION PAGE

Form Approved
OMB No. 0704-0188

1. AGENCY USE ONLY *(Leave blank)*	2. REPORT DATE August 1998	3. REPORT TYPE AND DATES COVERED Final	

4. TITLE AND SUBTITLE

USE OF THE INSTRUMENTED BOLT AND CONSTANT
DISPLACEMENT BOLT-LOADED SPECIMEN TO MEASURE
IN SITU HYDROGEN CRACK GROWTH IN HIGH STRENGTH STEELS

5. FUNDING NUMBERS

AMCMS No. 6111.01.91A1.100

6. AUTHOR(S)

Gregory N. Vigilante, John H. Underwood, and Daniel Crayon

7. PERFORMING ORGANIZATION NAME(S) AND ADDRESS(ES)

U.S. Army ARDEC
Benet Laboratories, AMSTA-AR-CCB-O
Watervliet, NY 12189-4050

8. PERFORMING ORGANIZATION REPORT NUMBER

ARCCB-TR-98015

9. SPONSORING/MONITORING AGENCY NAME(S) AND ADDRESS(ES)

U.S. Army ARDEC
Close Combat Armaments Center
Picatinny Arsenal, NJ 07806-5000

10. SPONSORING/MONITORING AGENCY REPORT NUMBER

12a. DISTRIBUTION/AVAILABILITY STATEMENT

Approved for public release; distribution unlimited.

12b. DISTRIBUTION CODE

13. ABSTRACT *(Maximum 200 words)*

Aggressive environments experienced by large caliber gun tubes during processing and firing have lead to a great deal of investigation on the hydrogen-induced cracking susceptibility of high strength steels. The constant displacement bolt-loaded specimen has been used to determine the hydrogen crack growth rates and threshold stress intensity of AF1410—both conventionally and isothermally heat treated—and AerMet 100. Additionally, the severe susceptibility of high strength steels has necessitated the application and modification of a low cost, highly reliable, in situ crack measurement method, called the instrumented bolt. The instrumented bolt consists of a full bridge, strain-gaged stainless steel bolt coupled to an automatic data acquisition system. New expressions have been developed for use with the instrumented bolt and bolt-loaded specimen to relate load to crack growth. Our study determined that Stage II crack growth rates for the AF1410 were $1.1E^{-2}$ and $2.3E^{-2}$ mm/s for conventional and isothermal AF1410, respectively. Threshold stress intensity levels for AF1410 were 16.0 and 13.7 MPa $m^{1/2}$, respectively. Stage II crack growth rates for AerMet 100 were $2.4E^{-2}$ mm/s, while the threshold stress intensity was 14.1 MPa $m^{1/2}$.

14. SUBJECT TERMS

Hydrogen-Induced Cracking, Hydrogen Embrittlement, Environmental Cracking, Environmental Fracture, Instrumented Bolt, Bolt-Loaded Specimen, High Strength Steels, ASTM A723, AF1410, AerMet 100

15. NUMBER OF PAGES

23

16. PRICE CODE

17. SECURITY CLASSIFICATION OF REPORT	18. SECURITY CLASSIFICATION OF THIS PAGE	19. SECURITY CLASSIFICATION OF ABSTRACT	20. LIMITATION OF ABSTRACT
UNCLASSIFIED	UNCLASSIFIED	UNCLASSIFIED	UL

TABLE OF CONTENTS

TABLES

LIST OF ILLUSTRATIONS

i

ACKNOWLEDGEMENTS

BACKGROUND

Hydrogen-induced cracking has been a particular problem in armament applications because of the use of aggressive manufacturing environments (ref 1) and developmental propellants (refs 2, 3). Also, to meet the battlefield demands of increased range and muzzle velocity, higher yield strength gun tube materials are being developed. Ultimately this will result in a greater susceptibility of these materials to hydrogen-induced cracking. Of course, hydrogen-induced cracking is not a problem isolated to armament applications, but it is also a persistent problem in a variety of other industries including the welding, chemical, paper processing, oil and gas, and aerospace industries.

Previous hydrogen cracking studies were conducted on ASTM A723 steel using the constant displacement bolt-loaded compact specimen (ref 4). Stage II crack growth rates (da/dt) increased by approximately an order of magnitude from 10^{-5} mm/s to 10^{-4} mm/s upon increasing the yield strength from 1130 MPa to 1275 MPa. This work was recently investigated further to determine the hydrogen cracking susceptibility of A723 steel at yield strengths up to 1380 MPa. Under identical test conditions, results again demonstrated a dramatic correlation between yield strength and crack growth rates. In fact, for only a 22% increase in yield strength from 1130 MPa to 1380 MPa, Stage II da/dt increased by approximately 300-fold (Figure 1).

The rapid crack growth rates observed with A723 steel necessitated development of an in situ crack growth technique, since even higher strength materials (i.e., AF1410 and AerMet 100) were to be tested. Before the in situ crack measurement technique was developed, crack measurements were laboriously taken using an optical microscope. Initially, both the direct current potential drop (DCPD) and instrumented bolt techniques were pursued. However, with the DCPD method, significant underestimation of crack length occurred. This was attributed to electrical shorting between the pin and the bolt and/or shorting between the crack surfaces (ref 5). Consequently, instrumented bolts were investigated because of their low cost and relative ease of use.

A comprehensive literature review was performed to determine previous environmental cracking investigations using the bolt-loaded specimen and instrumented bolt. Surprisingly, the only published investigations of environmental cracking using the bolt-loaded specimen and instrumented bolt were by Chung et al. (refs 6, 7), who conducted stress corrosion cracking studies on sensitized 304 stainless steel at elevated temperatures.

MATERIALS, HEAT TREATMENTS, AND TEST ENVIRONMENT

AF1410 and AerMet 100 steels were tested in this investigation to demonstrate the instrumented bolt technique. AF1410 is an Air Force developed iron-cobalt-nickel alloy noted for its high strength and high toughness. AF1410 is strengthened by the martensite transformation, as well as formation of coherent chromium and molybdenum carbides (ref 8).

1

AF1410 was tested in the conventional heat-treated condition, as well as the isothermally-processed condition. The ASTM grain size number of conventionally heat-treated AF1410 was approximately 10.8. Previous work conducted by Vigilante et al. (ref 9) demonstrated that the producibility of AF1410 could be greatly improved through molten salt isothermal processing, wherein a mixture of bainite and martensite is formed. Initial tests determined no significant changes in the mechanical properties of AF1410 containing this microstructure. The ASTM grain size number of the isothermally-processed AF1410 was approximately 10.7. AerMet 100 is the commercially available version of AF1410, and has even higher strength due to an increase in the carbon, chromium, and molybdenum content for additional precipitation hardening. AerMet 100 is used in critical applications where ultrahigh strength and high toughness are essential, such as in military aircraft landing gear. The ASTM grain size number of the AerMet 100 tested was approximately 11.1. Tables 1 and 2 list material chemistry and pertinent physical and mechanical property data for these steels and Table 3 lists heat treatment information.

A concentrated 50% H_2SO_4 /50% H_3PO_4 solution by volume (pH ~1) was used to generate hydrogen in all of the tests conducted. This solution has been used in prior work to promote rapid hydrogen cracking in high strength steels and nickel-iron superalloys (ref 4).

TEST PROCEDURE

Constant Displacement Bolt-Loaded Compact Specimen

The 0.486 H/W constant displacement bolt-loaded compact specimen was used for all tests (Figure 2). The W dimension was 50.8 mm for these specimens. The thickness of the specimens was 0.375 W rather than 0.50 W in order to increase the applied stress intensity while remaining within the maximum load capacity of the instrumented bolt. Since these materials are highly susceptible to hydrogen-induced cracking (low K_{IHIC}), a small reduction in the thickness will not affect the validity of the test to meet plane-strain requirements. All bolt-loaded specimens were fatigue precracked at stress intensity levels less than 75% of applied stress intensity during hydrogen cracking testing. In order to reduce the applied load, all specimens were tested at either initial applied stress intensity levels of 55 MPa $m^{1/2}$ or 82 MPa $m^{1/2}$ and were tested with an initial a/W of approximately 0.5. Test durations using the instrumented bolt were typically 1 to 2 hours. As discussed below, this was more than enough time to achieve significant cracking and to reach the threshold stress intensity, K_{IHIC}, in these materials. However, for more accurate threshold measurements, additional specimens were tested with standard bolts for longer durations, typically 1000 hours. After test termination, each specimen was manually overloaded to expose the fracture surfaces. The remaining ligament was measured using a machinist's microscope to determine K_{IHIC}. The fracture surfaces were examined using a scanning electron microscope to characterize the fracture morphology.

Instrumented Bolt

Instrumented bolts are commonly used to measure tensile loads for a variety of different applications. However, with the constant displacement bolt-loaded specimen, the bolts undergo compressive loading. Several ½-20 UNF instrumented bolts were fabricated for these tests out of 17-4 PH martensitic stainless steel (H1025 condition). The bolts were instrumented with a full bridge strain gage 9.525 mm (3/8 in.) from the end of the bolt and they had a load bearing capacity of 44.5 kN (10,000 lbs.). A drawing of the instrumented bolt is shown in Figure 3. The cost of each bolt was less than five hundred dollars, thus providing a cost effective technique to measure in situ crack growth.

The instrumented bolt was mounted into a servo-hydraulic mechanical test machine to determine the accuracy of the bolt. The load output (mv) from the instrumented bolt was compared to the load cell output from the mechanical test machine at 4.5 kN (1000 lb.) intervals from 4.5 to 40 kN (9000 lbs.). The load from the instrumented bolt was accurate to ±155 N (35 lbs.) and was repeatable to ±45 N (10 lbs.) over the full range of load tested. In addition, the load output from the instrumented bolt was compared to the theoretical v/P expressions for the 0.486 H/W bolt-loaded specimen at a/W of 0.3 to 0.9. Care was taken to ensure that both the pin hole and the bolt hole were parallel and perpendicular within 0.0254 mm of reference surfaces. A hardened hemispherical ball bearing was used between the pin and the instrumented bolt to facilitate point contact and alignment. At all a/W, the load from the instrumented bolt was measured and the drop in load was monitored with time as the crack advanced. A 12-bit resolution analog/digital (A/D) plug-in card monitored the instrumented bolt output. To improve sensitivity, the gain on the acquisition software was maximized. The floating error with the data acquisition system was ±135 N (30 lbs.).

v/P, K/P, and a/W Expressions

The wide range expression for K/v versus a/W used with the bolt-loaded specimen tests here was recently published by Underwood et al. (ref 1). This is also the expression used for the ongoing incorporation of the bolt-loaded specimen into ASTM Method 1681 for environmentally-assisted cracking tests on metallic materials. The expression is

$$KW^{1/2}/Ev(1-a/W)^{1/2} = 0.654 - 1.88(a/W) + 2.66(a/W)^2 - 1.233(a/W)^3 \qquad (1)$$

$$for \ X/W = 0.255, \ H/W = 0.486, \ 0.3 \ge a/W \ge 1.0$$

3

However, for instrumented bolt tests, additional expressions for K/P and v/P versus a/W are necessary to determine stress intensity and crack growth from the load output of the instrumented bolt. Figure 4 summarizes some available K/P versus a/W results for the bolt-loaded specimen as well as a new K/P expression developed here. Newman's numerical data used by Lisagor are shown, along with the plot of Lisagor's expression fitted to the Newman data (ref 9). Using the deep-crack bending limit K solution (ref 11), it can be shown that the limit of the K/P expression in the form here is

$$\lim_{a/W \to 1}[KBW^{1/2}/P(1 - a/W)^{3/2}/(2 + a/W)] = 1.325 \tag{2}$$

Note that the Lisagor expression does not approach the deep-crack limit. The expression of Saxena and Hudak (ref 12) properly approaches the deep-crack limit, but it deviates from the Newman data at small a/W, because apparently it was fitted to earlier Newman data that did not represent the bolt and pin configuration as well as the later data used here. The K/P expression developed here is

$$(KBW^{1/2}/P(1 - a/W)^{3/2}/(2 + a/W) = 1.515 + 3.22(a/W) -$$
$$12.76(a/W)^2 + 15.17(a/W)^3 - 5.82(a/W)^4 \tag{3}$$

for X/W = 0.255, H/W = 0.486, 0.2 ≥ a/W ≥ 1.0

This expression fits the Newman data within 0.6%, except for a/W = 0.9, where the fit is within 1.5%. However, the 1.5% difference at a/W = 0.9 can be disregarded, considering that the expression fits the deep-crack limit within 0.1% and that numerical methods at high a/W can be in error.

An a/W versus v/P expression is useful with instrumented bolt specimens to calculate crack length and crack growth rates from load values as the test proceeds. Using the deep-crack bending limit angular displacement solution (ref 12),

$$\theta = 15.80 \, M/EB(W - a)^2 \tag{4}$$

4

The relationships M = PW and θ = v/(W+X), which hold at the deep-crack limit, are

$$(vEB/P)(1 - a/W)^2 = 15.80(1 + X/W) \qquad \qquad (5)$$

Equation (5) shows that an expression in the form a/W = *function* $[1/(vEB/P)^{1/2}]$ would be expected to provide a good fit of the data. The expression developed using this form is shown in Figure 5 and is given as

$$a/W = 1 - 3.91Z - 4.77Z^2 + 32.03Z^3 \qquad \qquad (6)$$

where $Z = 1/(vEB/P)^{1/2}$, $X/W = 0.255$, $H/W = 0.486$, $0.3 \geq a/W \geq 1.0$

Using equation (6) with (vEB/P) from the Newman numerical data, the calculated a/W is within 0.003 of the actual values of a/W.

The expressions of equations (1), (3), and (6) were used to calculate crack-mouth displacement, load, and crack length for the bolt-loaded compact specimen tests described here. The new expressions, equations (3) and (6), are particularly useful for determining crack growth rate, da/dt, using an instrumented bolt.

RESULTS AND DISCUSSION

Crack Growth Rates, da/dt, and Threshold Stress Intensities, K_{IHIC}

As mentioned earlier, test durations of only a few hours were sufficient to achieve deep cracking and K_{IHIC} limits. $K_{applied}$ versus time for A723 (1380 MPa yield strength), AF1410, and AerMet 100 tests are shown in Figure 6. This figure dramatically illustrates the rapid hydrogen crack advance in these materials, as well as the need for in situ crack measurement techniques such as the instrumented bolt.

Stage II da/dt values for conventionally processed AF1410 were approximately $1.1E^{-2}$ mm/s compared to $2.3E^{-2}$ mm/s for the isothermally processed AF1410 (Figure 7). Threshold stress intensity values for the conventionally processed AF1410 were approximately 16 MPa m$^{1/2}$ compared to approximately 13.7 MPa m$^{1/2}$ for the isothermally processed AF1410. The increase in susceptibility of the isothermally processed AF1410 could be attributed to pockets of metastable retained austenite ahead of the crack tip that transforms into a highly susceptible martensitic microstructure; however, this was not confirmed.

5

The stage II da/dt values for the AerMet 100 specimens were approximately $2.4E^{-2}$ mm/s (Figure 7). This is much higher than the Stage II da/dt of $2.0E^{-5}$ mm/s measured by Atrens and reported by Graves (ref 13) in 3.5% NaCl. The hydrogen crack growth rates were believed to be higher simply because the acid environment used for these tests is a much more aggressive environment. The threshold stress intensity of the AerMet 100 specimens tested was approximately 14.1 MPa $m^{1/2}$. The hydrogen-cracked fracture morphology of the AF1410 specimens, both conventional and isothermal, was predominantly intergranular, while the remaining ligament was ductile (microvoid coalescence). The hydrogen-cracked fracture morphology of the AerMet 100 specimens tested was both transgranular and intergranular. The remaining ligament, however, was entirely microvoid coalescence. The fractographs of AF1410 and AerMet 100 specimens can be found in Figures 8 and 9.

Instrumented Bolt

A/D conversion errors affected post-test analysis in the Stage I portion of cracking. The slow crack advance in these regions, coupled with a relatively high sampling rate, resulted in fluctuations in the load measurement. For example, Figure 7 shows the conventional AF1410 data that caused initial errors in da/dt analysis. These errors were mitigated by the use of a ten point (or less) moving average of the data and by a decrease in the sampling rate.

The inherent errors in the instrumented bolt and in the 12-bit A/D converter card had a minimal effect on the crack length measurement. Under the test conditions used in this work, at the initial $K_{applied}$ (a/W = 0.5), a 155 N error resulted in only a 0.05-mm error in crack length. However, at deeper cracks (a/W = 0.9), a 155 N error resulted in a 0.3-mm error in crack length. These errors could be further reduced from ±155 N to ±8 N by using a 16-bit card rather than a 12-bit card in the data acquisition electronics.

When using an instrumented bolt with a bolt-loaded specimen, the discrepancy between the load from the instrumented bolt and the predicted load from the bolt-loaded specimen expressions is believed to be a fundamental problem. This is a logical conclusion since

- The load from the instrumented bolt was known to be accurate when compared to a mechanical tester in near perfect alignment;

- The pin and bolt holes in the bolt-loaded specimen were precisely machined;

- A point contact was made between the instrumented bolt and the pin in the bolt-loaded specimen.

The source of error is believed to be caused by two aspects of the instrumented bolt and bolt-loaded specimen configurations. First, the bolt-loaded specimen is asymmetric and the loading arms bend during application of the load. This results in misalignment between the axis of the instrumented bolt and the axis of the load applied to the end of the bolt. Second, because of the close proximity of the strain gage to the end of the bolt, the strain gage output is affected by the misalignment between the bolt and load axes. The result is an underestimation of the load in the bolt-loaded specimen by approximately 20%.

SUMMARY AND CONCLUSIONS

1. Rapid Stage II hydrogen crack growth rates in high strength steels necessitated the development of a low cost, reliable in situ crack measurement technique, the instrumented bolt.

2. A ½-20 UNF bolt instrumented with a full bridge strain gage was coupled to an automatic data acquisition system to measure and record in situ hydrogen crack growth.

3. In order to fully utilize the capabilities of the instrumented bolt and bolt-loaded specimen, new expressions were developed for K/P versus a/W and a/W versus v/P.

4. The load measured from the instrumented bolt was approximately 20% less than the predicted load from expressions for the bolt-loaded specimen. This was overcome by calibrating the load data accordingly after test termination. The discrepancy in load is a fundamental problem with the configuration of the bolt-loaded specimen due to bending in its loading arms coupled with the proximity of the strain gage to the end of the instrumented bolt.

5. AF1410 and AerMet 100, two ultrahigh strength steels, were used to demonstrate the capabilities of the instrumented bolt. In addition, a new isothermal heat treatment of AF1410 was tested to characterize the material's hydrogen embrittlement susceptibility.

6. The Stage II crack growth rates of isothermal and conventional AF1410 were 1.1E^{-2} mm/s and 2.3E^{-2} mm/s, respectively. The threshold stress intensity levels of the two heat treatments of AF1410 were 16.0 MPa m$^{1/2}$ and 13.7 MPa m$^{1/2}$, respectively. The Stage II crack growth rates of the AerMet 100 material were 2.4E^{-2} and the threshold stress intensity was 14.1 MPa m$^{1/2}$.

REFERENCES

1. Underwood, J.H., Olmstead, V.J., Askew, J.C., Kapusta, A.A., and Young, G.A., "Environmentally Controlled Fracture of an Overstrained A723 Steel Thick-Wall Cylinder," *Fracture Mechanics: Twenty-Third Symposium, ASTM STP 1189*, (Ravinder Chona, Ed.), American Society for Testing and Materials, Philadelphia, 1993, pp. 443-460.

2. Troiano, E., Underwood, J.H., O'Hara, G.P., and Crayon, D., "Fatigue Analysis of a Pressure Vessel Experiencing Pressure Oscillations," *Fatigue and Fracture Mechanics: 28th Volume, ASTM STP 1321*, (J.H. Underwood, B.D. MacDonald, and M.R. Mitchell, Eds.), American Society for Testing and Materials, West Conshohocken, PA, 1997.

3. Underwood, J.H., Parker, A.P., Cote, P.J., and Sopok, S., "Compressive Thermal Yielding Leading to Hydrogen Cracking in a Fired Cannon," *Proceedings of ASME Pressure Vessels and Piping Conference*, San Diego, CA, 26-30 July 1998.

4. Vigilante, G.N., Underwood, J.H., Crayon, D., Tauscher, S., Sage, T., and Troiano, E., "Hydrogen-Induced Cracking Tests of High-Strength Steels and Nickel-Iron Base Alloys Using the Bolt-Loaded Specimen," *Fatigue and Fracture Mechanics: 28th Volume, ASTM STP 1321*, (J.H. Underwood, B.D. MacDonald, and M.R. Mitchell, Eds.), American Society for Testing and Materials, West Conshohocken, PA, 1997.

5. Landes, J.D., and Wei, R. P., "The Kinetics of Subcritical Crack Growth Under Sustained Loading," *International Journal of Fracture*, Vol. 9, No. 3, September 1973, pp. 277-293.

6. Chung, P., Yoshitake, A., Cragnolino, G., and MacDonald, D.D., "Environmentally-Controlled Crack Growth Rate of Type 304 Stainless Steel in High Temperature Sulfate Solutions," *Corrosion '84*, Paper No. 166, New Orleans, LA, 1984.

7. Chung, P.C., Cragnolino, G., and MacDonald D.D., "Instrumented Loading Devices for Monitoring Environmentally Assisted Crack Growth in High Temperature Aqueous Systems," *Corrosion-NACE*, Vol. 41, No. 3, March 1985.

8. Unimach AF-1410 High Strength Steel Technical Data Sheet, Universal-Cyclops Specialty Steel Division, Pittsburgh, PA, 1978.

9. Vigilante, G.N., Cote, P.J., Hickey, T., and Pan, S.K., "Isothermal Bainite in AF1410," ARDEC Technical Report ARCCB-TR-96012, Benet Laboratories, Watervliet, NY, April 1996.

10. Lisagor, W.B., "Influence of Precracked Specimen Configuration and Starting Stress Intensity on the Stress Corrosion Cracking of 4340 Steel," *Environment-Sensitive Fracture: Evaluation and Comparison of Test Methods, ASTM STP 821*, American Society for Testing and Materials, Philadelphia, 1984, pp. 80-97.

11. Tada, H., Paris, P.C., and Irwin, G.R., *The Stress Analysis of Cracks Handbook*, Paris Productions, Inc., St. Louis, MO, 1985, p. 9.1.

12. Saxena, A., and Hudak, S.J., Jr., "Review and Extension of Compliance Information for Common Crack Growth Specimens," *International Journal of Fracture*, Vol. 14, No. 5, 1978, pp. 543-468.

13. Graves, J.H., "Effect of Heat Treatment on the Microstructure and Properties of AerMet 100 Steel," Army Research Laboratory Technical Report ARL-TR-507, Watertown, MA, August 1994.

**Table 1. Material Chemistry for AF1410 and AerMet 100
(Wt. %)**

Element	AF1410	AerMet 100
Carbon	0.13-0.17	0.21-0.25
Cobalt	13.5-14.5	13.0-14.0
Nickel	9.5-10.5	11.0-12.0
Chromium	1.8-2.2	2.9-3.3
Molybdenum	0.90-1.10	1.1-1.3
Manganese	0.10 max.	0.10 max.
Sulfur	0.005 max.	0.005 max.
Phosphorous	0.008 max.	0.008 max.
Titanium	0.015 max.	0.015 max.
Iron	Balance	Balance

Table 2. Pertinent Physical and Mechanical Properties

Property	AF1410 Conventional	AF1410 Isothermal	AerMet 100
Young's Modulus, E (GPa)	203	203	193
0.2% Yield Strength (MPa)	1551	1530	1725
Fracture Toughness, K_{max} (MPa m$^{1/2}$)	172	187	127

Table 3. Heat Treatments Employed

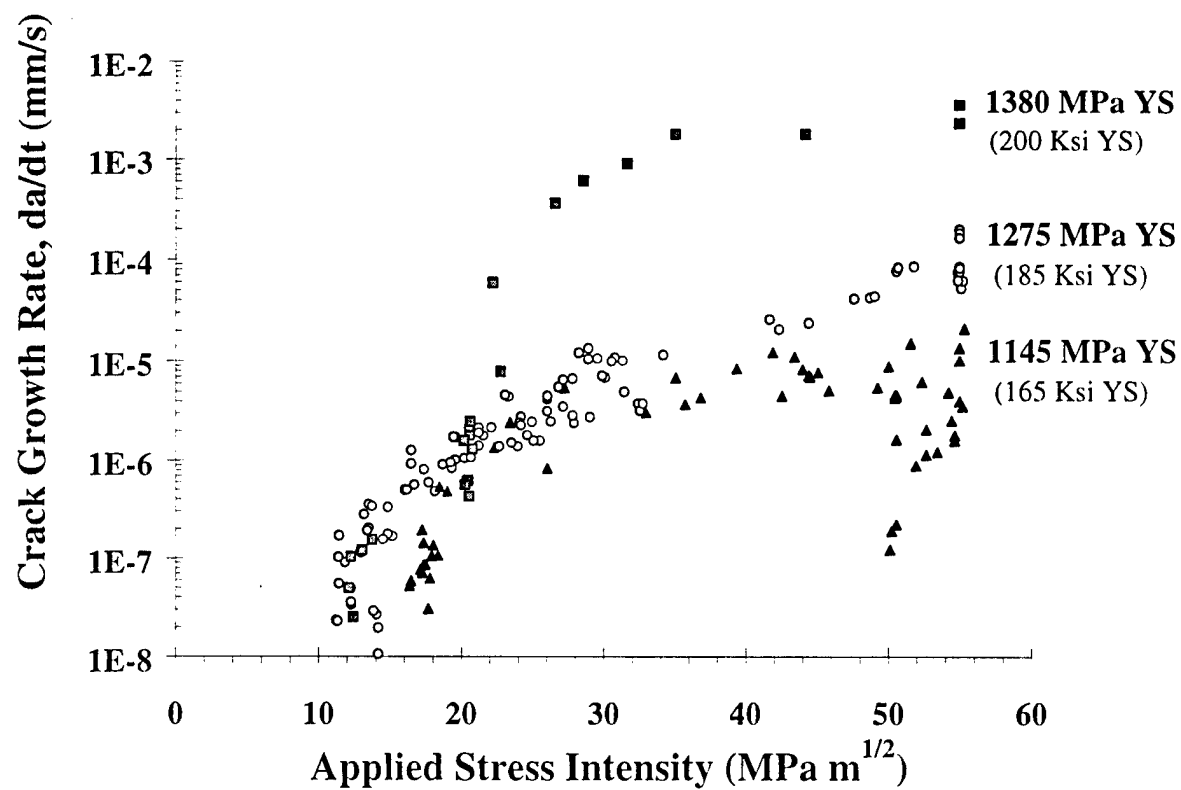| Material	Heat Treatment
AF1410 Conventional	900°C 1 hour, air cool 840°C 1 hour, air cool Age 510°C 5 hours, air cool
AF1410 Isothermal	900°C 1 hour, air cool 840°C 1 hour, air cool to 300°C Isothermal hold for 1 hour, air cool Age 510°C 5 hours, air cool
AerMet 100	885°C 1 hour, oil quench Refrigerate at -73°C 1 hour, air warm Age 482°C 5 hours, air cool

Figure 1. Effect of increasing yield strength on crack growth rates in ASTM A723 steel.
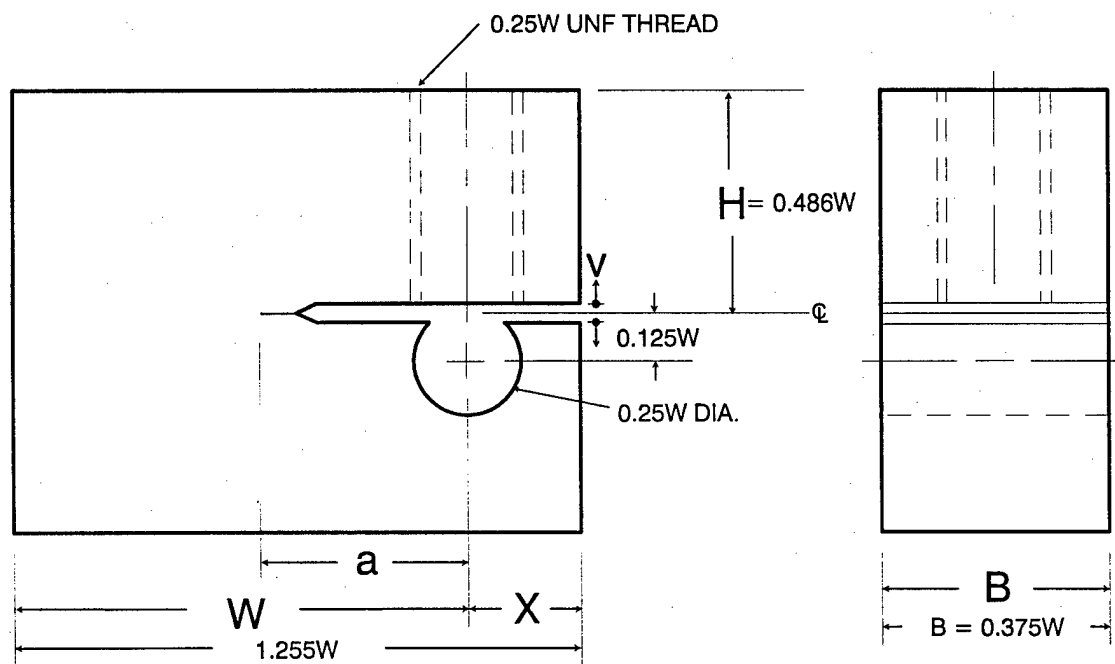
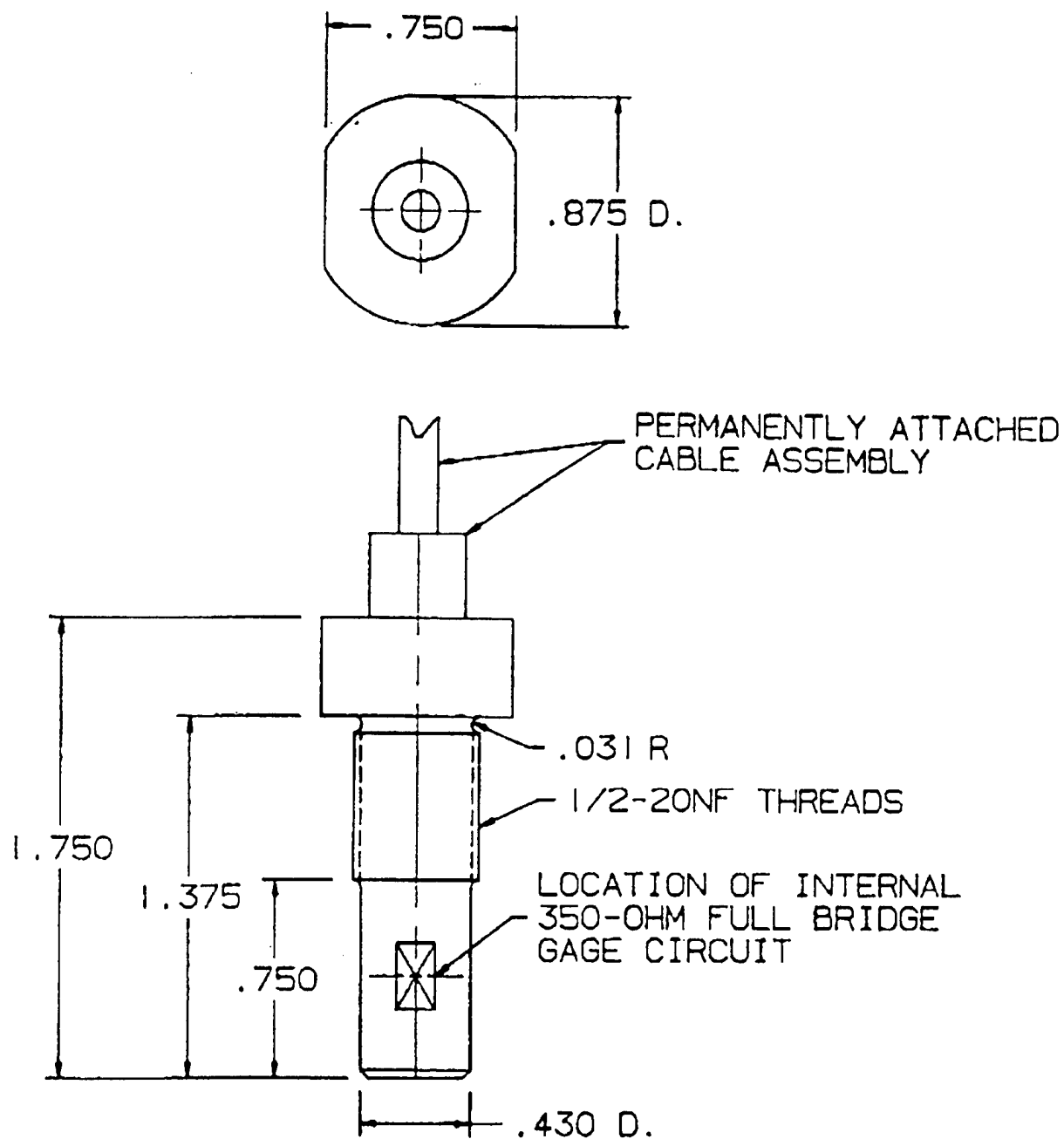Figure 2. 0.486 H/W bolt-loaded specimen.

Figure 3. 17-4 PH stainless steel instrumented bolt; note English units.
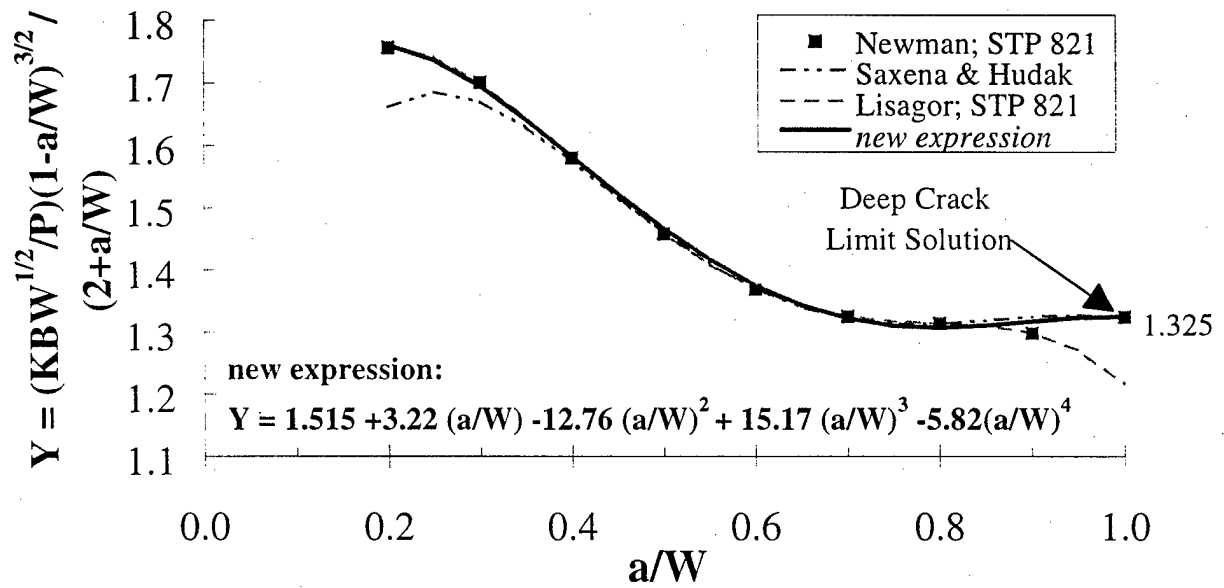(Printed with permission from Strainsert Company, West Conshohocken, PA.)

Figure 4. New K/P versus a/W expression for the 0.486 H/W bolt-loaded specimen.

The y-axis is labeled $Y = (KBW^{1/2}/P)(1-a/W)^{3/2} / (2+a/W)$ and the x-axis is labeled a/W.

Legend:
- Newman; STP 821
- Saxena & Hudak
- Lisagor; STP 821
- *new expression*

Deep Crack Limit Solution

1.325

new expression:

$$Y = 1.515 + 3.22\,(a/W) - 12.76\,(a/W)^2 + 15.17\,(a/W)^3 - 5.82(a/W)^4$$
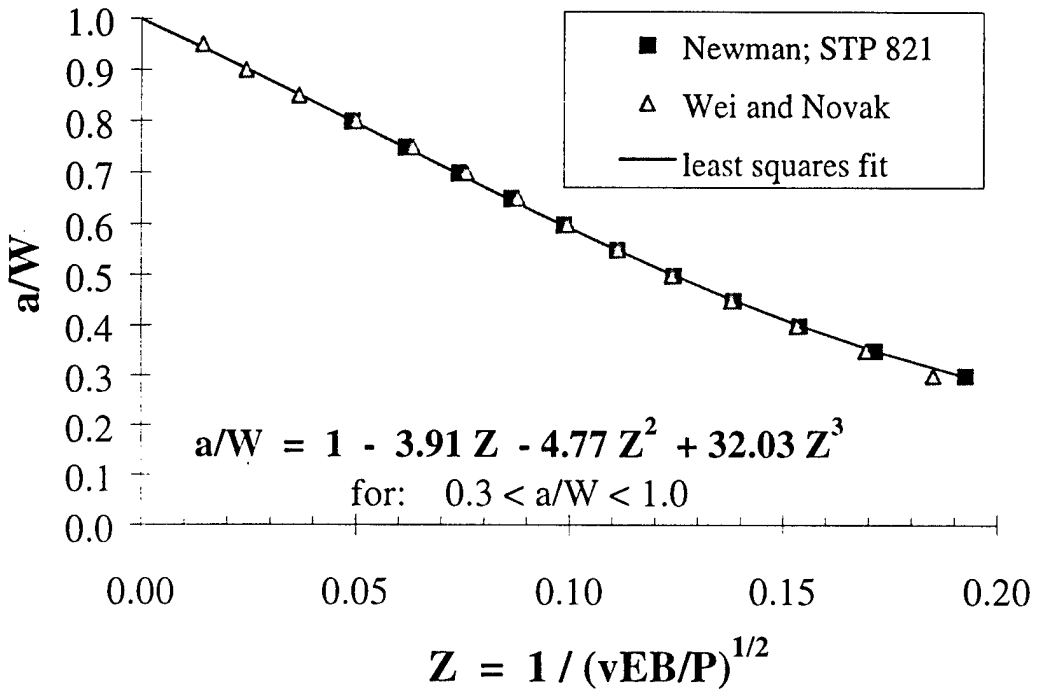
Figure 5. New a/W versus v/P expression for the 0.486 H/W bolt-loaded specimen.

The figure shows a plot with y-axis labeled a/W (ranging 0.0 to 1.0) and x-axis labeled $Z = 1/(vEB/P)^{1/2}$ (ranging 0.00 to 0.20). Legend indicates: ■ Newman; STP 821, △ Wei and Novak, — least squares fit.

$$a/W = 1 - 3.91\ Z - 4.77\ Z^2 + 32.03\ Z^3$$
$$\text{for:}\quad 0.3 < a/W < 1.0$$
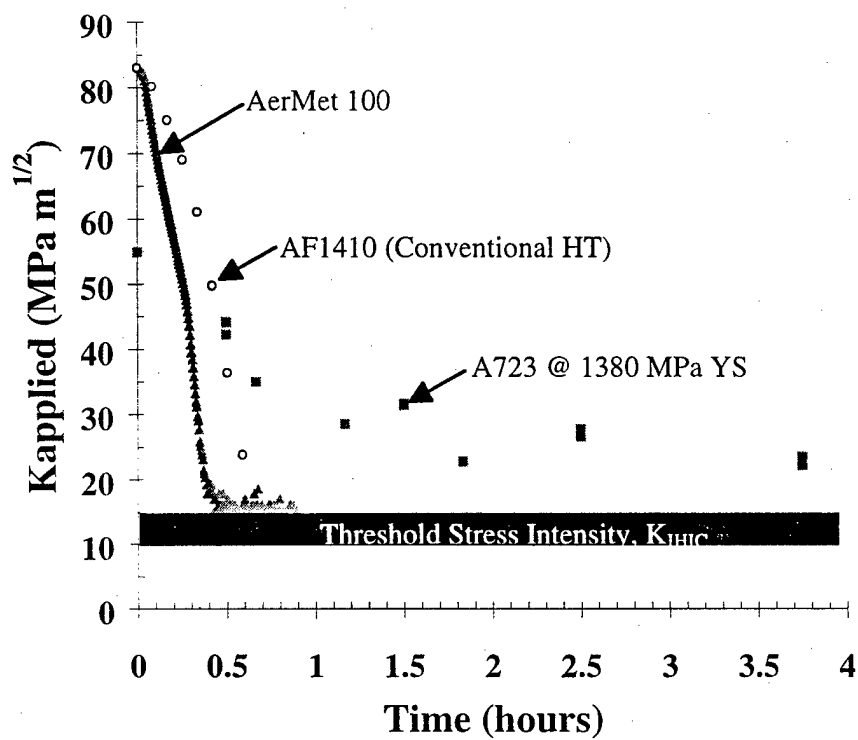
Figure 6. Representative $K_{applied}$ versus time data for A723, AF1410, and AerMet 100; bolt-loaded specimen tested in H_2SO_4/H_3PO_4 acid.
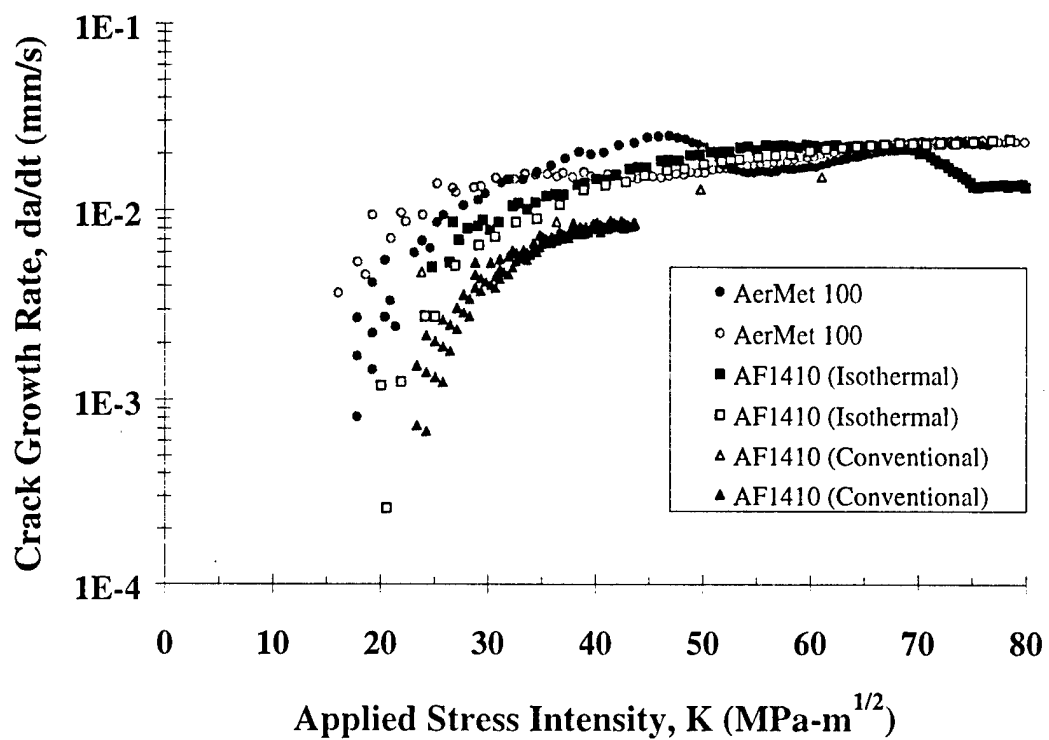
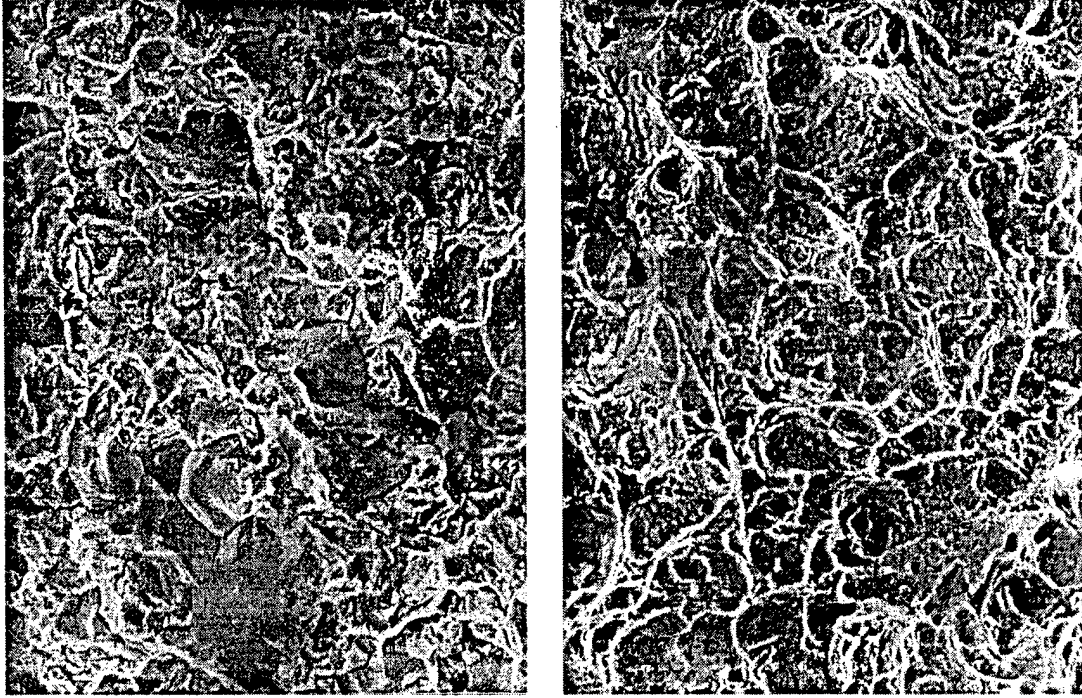Figure 7. da/dt data on AF1410 and AerMet 100 using the instrumented bolt.

Figure 8. Morphology of the hydrogen-cracked portion of AF1410, both
conventional and isothermal, showing predominantly intergranular structure
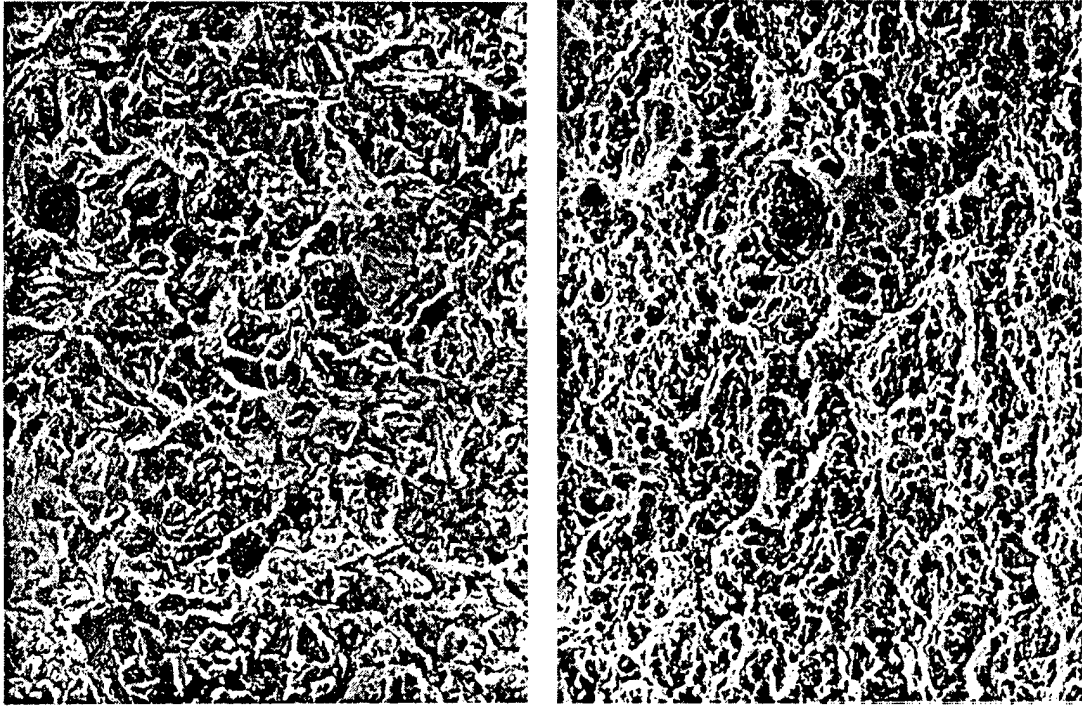on left with the remaining ligament entirely ductile on right (magnification 500X).

Figure 9. Morphology of hydrogen-cracked region of AerMet 100 showing intergranular and transgranular structure on left with the remaining ligament entirely ductile on right (magnification 500X).

TECHNICAL REPORT INTERNAL DISTRIBUTION LIST

	NO. OF COPIES
CHIEF, DEVELOPMENT ENGINEERING DIVISION	
ATTN: AMSTA-AR-CCB-DA	1
-DB	1
-DC	1
-DD	1
-DE	1
CHIEF, ENGINEERING DIVISION	
ATTN: AMSTA-AR-CCB-E	1
-EA	1
-EB	1
-EC	1
CHIEF, TECHNOLOGY DIVISION	
ATTN: AMSTA-AR-CCB-T	2
-TA	1
-TB	1
-TC	1
TECHNICAL LIBRARY	
ATTN: AMSTA-AR-CCB-O	5
TECHNICAL PUBLICATIONS & EDITING SECTION	
ATTN: AMSTA-AR-CCB-O	3
OPERATIONS DIRECTORATE	
ATTN: SIOWV-ODP-P	1
DIRECTOR, PROCUREMENT & CONTRACTING DIRECTORATE	
ATTN: SIOWV-PP	1
DIRECTOR, PRODUCT ASSURANCE & TEST DIRECTORATE	
ATTN: SIOWV-QA	1

NOTE: PLEASE NOTIFY DIRECTOR, BENÉT LABORATORIES, ATTN: AMSTA-AR-CCB-O OF ADDRESS CHANGES.

TECHNICAL REPORT EXTERNAL DISTRIBUTION LIST

	NO. OF COPIES		NO. OF COPIES

ASST SEC OF THE ARMY
RESEARCH AND DEVELOPMENT
ATTN: DEPT FOR SCI AND TECH — 1
THE PENTAGON
WASHINGTON, D.C. 20310-0103

COMMANDER
ROCK ISLAND ARSENAL
ATTN: SMCRI-SEM — 1
ROCK ISLAND, IL 61299-5001

DEFENSE TECHNICAL INFO CENTER
ATTN: DTIC-OCP (ACQUISITIONS) — 2
8725 JOHN J. KINGMAN ROAD
STE 0944
FT. BELVOIR, VA 22060-6218

COMMANDER
U.S. ARMY TANK-AUTMV R&D COMMAND
ATTN: AMSTA-DDL (TECH LIBRARY) — 1
WARREN, MI 48397-5000

COMMANDER
U.S. ARMY ARDEC
ATTN: AMSTA-AR-AEE, BLDG. 3022 — 1
    AMSTA-AR-AES, BLDG. 321 — 1
    AMSTA-AR-AET-O, BLDG. 183 — 1
    AMSTA-AR-FSA, BLDG. 354 — 1
    AMSTA-AR-FSM-E — 1
    AMSTA-AR-FSS-D, BLDG. 94 — 1
    AMSTA-AR-IMC, BLDG. 59 — 2
PICATINNY ARSENAL, NJ 07806-5000

COMMANDER
U.S. MILITARY ACADEMY
ATTN: DEPARTMENT OF MECHANICS — 1
WEST POINT, NY 10966-1792

U.S. ARMY MISSILE COMMAND
REDSTONE SCIENTIFIC INFO CENTER — 2
ATTN: AMSMI-RD-CS-R/DOCUMENTS
    BLDG. 4484
REDSTONE ARSENAL, AL 35898-5241

DIRECTOR
U.S. ARMY RESEARCH LABORATORY
ATTN: AMSRL-DD-T, BLDG. 305 — 1
ABERDEEN PROVING GROUND, MD
  21005-5066

COMMANDER
U.S. ARMY FOREIGN SCI & TECH CENTER
ATTN: DRXST-SD — 1
220 7TH STREET, N.E.
CHARLOTTESVILLE, VA 22901

DIRECTOR
U.S. ARMY RESEARCH LABORATORY
ATTN: AMSRL-WT-PD (DR. B. BURNS) — 1
ABERDEEN PROVING GROUND, MD
  21005-5066

COMMANDER
U.S. ARMY LABCOM, ISA
ATTN: SLCIS-IM-TL — 1
2800 POWDER MILL ROAD
ADELPHI. MD 20783-1145

NOTE: PLEASE NOTIFY COMMANDER, ARMAMENT RESEARCH, DEVELOPMENT, AND ENGINEERING CENTER,
BENÉT LABORATORIES, CCAC. U.S. ARMY TANK-AUTOMOTIVE AND ARMAMENTS COMMAND,
    AMSTA-AR-CCB-O. WATERVLIET, NY 12189-4050 OF ADDRESS CHANGES.

	NO. OF COPIES		NO. OF COPIES
COMMANDER U.S. ARMY RESEARCH OFFICE ATTN: CHIEF, IPO P.O. BOX 12211 RESEARCH TRIANGLE PARK, NC 27709-2211	1	WRIGHT LABORATORY ARMAMENT DIRECTORATE ATTN: WL/MNM EGLIN AFB, FL 32542-6810	1
DIRECTOR U.S. NAVAL RESEARCH LABORATORY ATTN: MATERIALS SCI & TECH DIV WASHINGTON, D.C. 20375	1	WRIGHT LABORATORY ARMAMENT DIRECTORATE ATTN: WL/MNMF EGLIN AFB, FL 32542-6810	1

NOTE: PLEASE NOTIFY COMMANDER, ARMAMENT RESEARCH, DEVELOPMENT, AND ENGINEERING CENTER, BENÉT LABORATORIES, CCAC, U.S. ARMY TANK-AUTOMOTIVE AND ARMAMENTS COMMAND, AMSTA-AR-CCB-O, WATERVLIET, NY 12189-4050 OF ADDRESS CHANGES.